NASA Technical Memorandum 101299

New Acousto-Ultrasonic Techniques Applied to Aerospace Materials

Harold E. Kautz
Lewis Research Center
Cleveland, Ohio

NASA

NEW ACOUSTO-ULTRASONIC TECHNIQUES APPLIED TO AEROSPACE MATERIALS

Harold E. Kautz
National Aeronautics and Space Administration
Lewis Research Center
Cleveland, Ohio 44135

ABSTRACT

The use of an NdYAG pulsed laser for generating ultrasonic waves for NDE in resin matrix composites was investigated. A study was conducted of the use of the 1.064 μm wavelength NdYAG pulsed laser with the neat, unreinforced resin as well as with graphite fiber/polymer composite specimens. In the case of neat resins it was found that, at normal incidence, about 25 percent of the laser pulse energy is reflected at the incident surface. An attenuation coefficient for the polymide resin, PMR-15 was determined to be ~5.8 np/cm. This means, for example, that for a 1/16 in. panel thickness 24 percent of the incident energy is transmitted through the panel. Under these conditions much of the laser produced ultrasonic wave will originate throughout the bulk of the specimen rather than at the surface in contrast to the case with piezoelectric transducers. It was found in energy balance studies that graphite fiber/polymer specimens attenuate the laser beam more than do the neat resins. The increased absorption is in the graphite fibers.

The occurrence of laser induced surface damage was also studied. For the polymer neat resin, damage appears as pit formation over a small fraction of the pulse impact area and discoloration over a larger part of the area. A damage threshold was inferred from observed damage as a function of pulse energy. The 600 °F cured PMR-15 and PMR-11 exhibit about the same amount of damage for a given laser pulse energy. The damage threshold is between 0.06 and 0.07 J/cm^2. In the case of graphite fiber/polymer specimens damage studies showed that the fibers burn away to the extent of partially shielding the resin from pit formation and discoloration.

Acousto-ultrasonic signals were collected with a piezoelectric transducer over a wide range of laser pulse energies. It was found that signal strengths typical of those produced by piezoelectric sending transducers can be achieved at laser pulse energies well below the damage threshold.

INTRODUCTION

The use of lasers for stimulation and detection of ultrasonic waves in materials is of high interest for nondestructive evaluation (Refs. 1 to 5). Automation of laser beam scanning seems considerably more practical than direct coupling of piezoelectric transducers to the surface. Thus remote scanning of large areas becomes viable.

1

New techniques usually present limitation along with their advantages, however. One serious limitation of lasers is likely to be their potential for doing damage to surfaces. Development of laser ultrasonics ought to include examination of the potential damage to materials that are of aerospace interest.

Acousto-ultrasonics is a two transducer NDE technique for assessing mechanical strength in composites. It has an advantage of allowing one-side access to structures. The application of lasers to injection of the ultrasonic signal (laser-in) and also to the detection (laser-out) can lead to better mechanization of acousto-ultrasonic scanning of large specimens.

The present work focuses on laser-in ultrasonics. Laser pulse energy damage thresholds are examined and compared for energy ranges that produce useful acousto-ultrasonic signals. This is done for neat polymeric resin panels and fiber reinforced polymer matrix composite laminate samples.

MATERIALS, EXPERIMENTAL, AND PROCEDURE

A schematic diagram of the laser system used for these experiments is shown in Fig. 1. The laser is a solid state NdYAG (Neodinium Ytterium Garnet) pulsed laser with 1.064 μm wavelength and filtered to provide pulses of various energy. The digitizing oscilloscope was controlled to collect single sweep acousto-ultrasonic signals with a PDP/1134 computer and store them on disc.
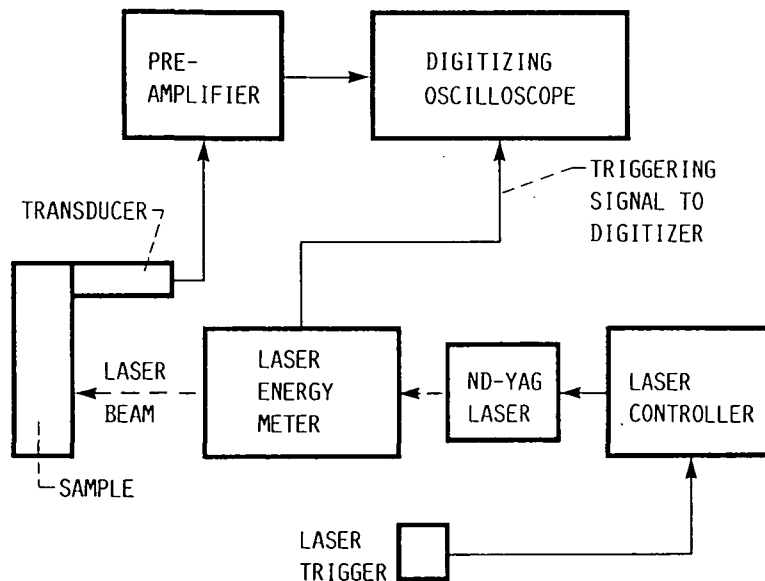
FIGURE 1. - SCHEMATIC OF LASER CALIBRATION AND MEASUREMENT SYSTEM.

Materials Studied

Table 1 lists the materials studied in these experiments. All were flat panels of various dimensions. The fiber-reinforced panels were composite laminates with ply orientations given in Table 1.

TABLE 1. Specimens studied

Material	Thickness, cm	Structure	Remarks, °F cure
PMR-15	0.145	Monolithic	600
PMR-15	.586	Monolithic	
PMR-11	.288	Monolithic	
Celion 6000/PMR-15	.533	28 ply 0/90	
Celion 6000/PMR-15	.550	30 ply uni-directional	
Celion 6000/PMR-11	.111	6 ply 0/45/ 90-center	

aPMR-15 is a polymide resin capable of service at 600 °F.
bPMR-11 is the same as PMR-15 except that it has lower
  molecular weight.
cCelion 6000 is a graphite fiber available from BASF.

Laser Damage Experiments

For the laser damage experiments positions on the surface of the speci-
men were repeatedly subjected to laser pulses of the same energy. Dif-
ferent positions received pulses at different energy levels but the
number of pulses were also varied so that the total energy at all posi-
tions was the same. For these experiments no acousto-ultrasonic meas-
urements were made.

Energy Balance Experiments

Energy transmitted through a specimen thickness was determined exper-
imentally by placing the specimen between the laser and the energy
meter in Fig. 1. Radiation energy meter readings were noted with the
specimen present and absent.

Acousto-ultrasonic Experiments

For these experiments the specimen was placed at the output of the energy
meter. A 1 MHz broad band transducer was coupled to the surface with
bee's wax, melted into place. In some cases, for comparison, specimens
were first excited by a 2.25 MHz broad band transducer before the laser-
in experiment. In each case waveform data were collected and stored on
disc for later examination of time domain waveform, frequency domain
spectrum, and for calculation of stress-wave factor (Ref. 6). The trans-
ducer excited signals reported here were all produced with the same
transducer, same pulser setting, and same geometry. The waveform digi-
tizer for these experiments is shown in Fig. 1.

ENERGY BALANCE CALCULATION

Figure 2 shows a schematic for the energy balance for a laser beam imping-
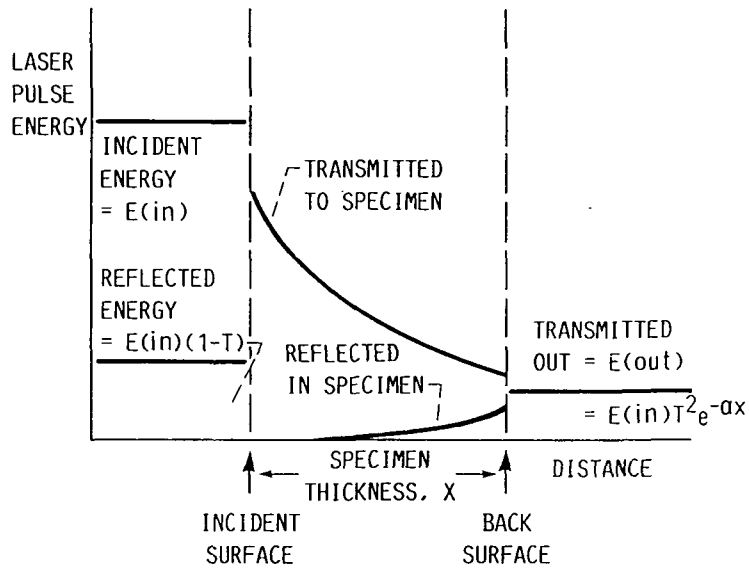ing at normal incidence on the surface of a specimen of thickness x.

FIGURE 2. - ENERGY BALANCE FOR LASER PULSE TRANSMITTED
THROUGH SPECIMEN.

Besides the specimen thickness, x, other measured quantities are the
energy of the incident beam at the front surface, E(in), and the energy
of the beam emerging from the back surface, E(out). These two energies
are related as follows.

$$E(out) = E(in)T(in)AT(out) \tag{1}$$

T(in) = transmission coefficient at the incident surface.
T(out) = transmission coefficient at back surface.
A = attenuation of beam through the thickness of the specimen.

It turns out that the transmission coefficient from a medium 1 to a
medium 2, (such as air to a composite), is the same as from medium 2
back into medium 1, (Ref. 7). There is a difference in what happens to
the phase of the wave but for our energy transmission coefficients at
the surface:

$$T(in) = T(out) = T \tag{2}$$

For the attenuation, A, within the specimen we assume Beer's law:

$$A = e^{(-\alpha x)} \tag{3}$$

A is a factor that multiplies the intensity at zero thickness which is
E(in)T of Eq. (1). "α" in Eq. (3) is the energy attenuation coefficient
with distance.

Equations (1), (2), and (3) can be combined as shown below.

$$E(out) = E(in)T^2 e^{(-\alpha x)} \tag{4}$$

Equation (4) contains two unknowns T and α. If one applies Eq. (4)
to data from two specimens that are identical except for thickness then
Eq. (4) can be used as simultaneous equations to yield values of T and
α. With this the energy balance can be calculated as below.

4

TABLE 2. Visible damage produced in PMR-15 neat resin material by
Nd-YAG 1.064 μm laser radiation

[T = Nne, E = ne.]

N	n	e	E	T	Observed damage
Number of pulse trains	Number of pulses in train	Energy density of pulse, J/cm^2	Energy density of train, J/cm^2	Total energy density on specimen, J/cm^2	
50	5	0.42	2.10	105	Pitting Nodules Discolored
298	1	.35	.35	104	Pitting Nodules Discolored
100	5	.208	1.04	104	Small Pit Nodules Discolored
192	5	.11	.55	106	No pitting Nodules No discolor
1189	1	.087	.087	103	No pitting Nodules No discolor
282	5	.074	.37	104	No pitting Few Nodules No discolor
369	5	.056	.28	103	No pitting No nodules No discolor

Total laser pulse energy(measured)   = E(in)
Energy reflected at incident surface = E(in)(1-T)
Energy absorbed in specimen   = E(in)T-E(out)
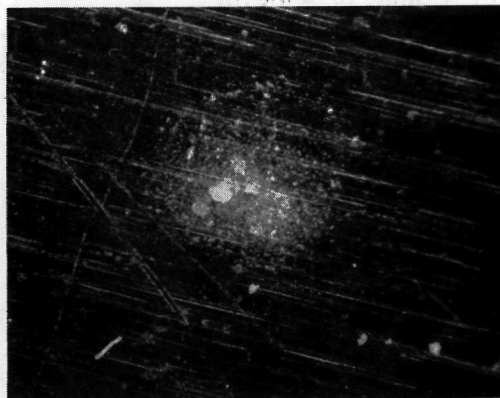Energy leaving back surface(measured) = E(out)

RESULTS

Laser Damage Experiments

Figures 3(a) to (b) show a sequence of laser radiated sites for a
0.145 cm thick PMR-15 panel at 50X magnification. Visible laser damage
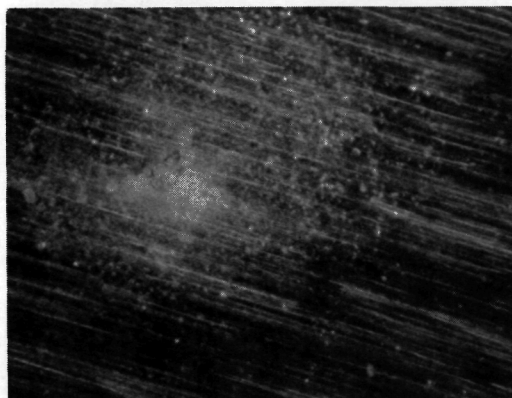
(a) 0.42 J/cm^2 PER PULSE.   (b) 0.21 J/cm^2 PER PULSE.

(c) 0.07 J/cm^2 PER PULSE.   (d) 0.06 J/cm^2 PER PULSE.

FIGURE 3. - LASER DAMAGE TO PMR-15 NEAT RESIN PRODUCED BY NdYAG PULSED LASER WITH CON-
TANT TOTAL DOSE.

was inferred from the presence of pitting, subsurface bubbles, and dis-
coloring that was not present elsewhere on the panel. The same results
are also described in Table 2. Each of the positions shown received
repeated pulses at a given energy. The number of repeats at each posi-
tion was chosen so that the damage at all positions could be compared
at about the same total dose of 104 to 105 J/cm^2. In Fig. 4 a
0.35 J/cm^2 per pulse level is show at 200X for greater detail.

Results for the 0.288 cm thick PMR-11 neat resin panel were the same as
for the PMR-15 presented in Figs. 3 and 4.

6

FIGURE 4. - VIEW OF DAMAGE FOR PMR-15 WITH 0.35 J/CM^2 PER PULSE.

Figures 5(a) to (d) show a sequence for the 28 ply composite panel of Celion 6000 graphite fibers and PMR-15 matrix for the same sequence of laser pulse energies as the Fig. 3 sequence for the neat resins alone.

Damage photos for these three panels should be compared with the same energy per pulse as follows:

Energy Balance Experiments

Among the specimen panels listed in Table 1 the two PMR-15 and the PMR-11 neat resin panels gave detectable levels of laser pulse energy exiting from the back surface. For these the ratio E(out)/E(in) was calculated. This was done for 6 to 8 pulse energy levels that spanned from below to above the observed damage threshold. The ratio did not vary significantly over this energy range. The averages for the panels with standard deviations is listed in Table 3.

In order to carry out an Eq. (4) calculation, the 0.145 cm thick and the 0.586 cm thick PMR-15 panels were assumed to have identical transmission coefficients and absorption coefficients. The result is:

Transmission coefficient T(air/PMR-15) = 0.750

absorption coefficient a(PMR-15)   = 5.78/cm.
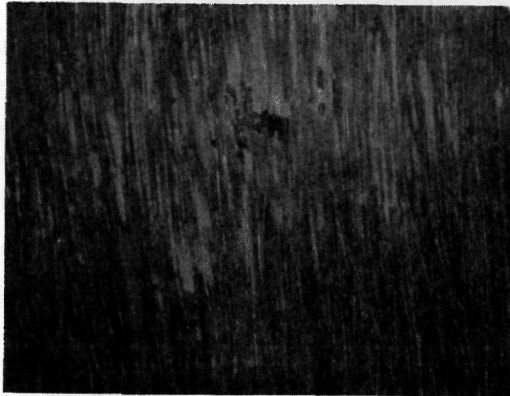
From this, the reflection coefficient R = 1-T = 0.25.

In Fig. 6 E(out)/E(in) is plotted against specimen thickness for the three neat resin panels. The line is constructed for the PMR-15 data used in the above calculation. The PMR-11 data point is also plotted for comparison.
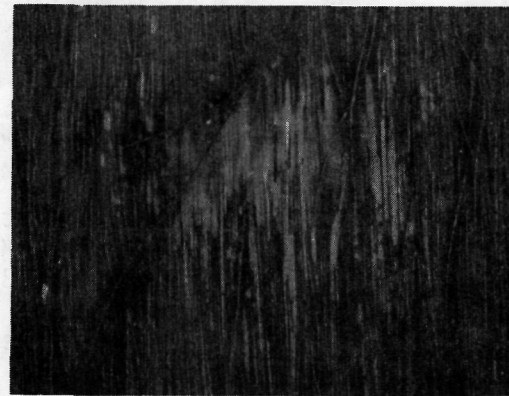
7
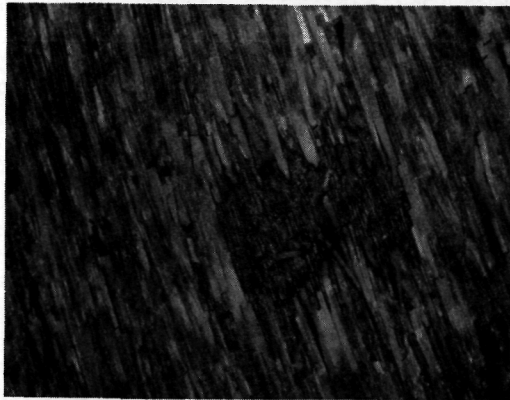
(a) 0.42 J/CM^2 PER PULSE.

(b) 0.21 J/CM^2 PER PULSE.

(c) 0.07 J/CM^2 PER PULSE.

(d) 0.06 J/CM^2 PER PULSE.

FIGURE 5. - LASER DAMAGE TO 28 PLY (0/90°) COMPOSITE WITH CELIUM 6000 FIBERS AND PMR-15 MATRIX (CONSTANT TOTAL DOSE).

TABLE 3. Energy balance data for PMR neat resin panels

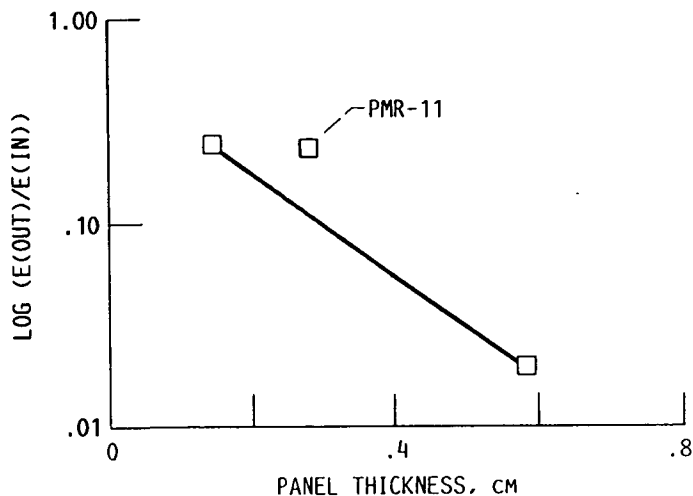| Material	Thickness, cm	Energy out/ energy in	Standard	Deviation, percent
PMR-15	0.145	0.243	0.008	3.3
PMR-15	.586	.0190	.0007	3.7
PMR-11	.288	.246	.003	1.2

8

FIGURE 6. - LOG OF E(OUT)/E(IN) VERSUS PANEL
THICKNESS FOR PMR 11 AND TWO PMR-15 NEAT
RESIN SPECIMENS.

No measureable E(out) pulse energy values were found for the graphite/
resin composite panels. This means that at the highest pulse energy
E(out)/E(in) was <1 percent, the limit of sensitivity for the energy
meter. This panel was free of visible voids or delaminations that
could effect the passage of the laser pulse.

Acousto-Ultrasonic Experiments

Figure 7 shows acousto-ultrasonic signals collected on the 0.145 cm
thick PMR-15 panel. Figure 7(a) is the time domain of a signal produced
by a 2.25 MHz broad band piezotransducer coupled to the panel through
an elastomer pad. Figure 7(b) is the frequency spectrum of 7(a).
Figure 7(c) is the time domain of a signal produced by a 0.030 mJ/cm^2
laser pulse. Figure 7(d) is the frequency spectrum of 7(c). Both wave-
forms in Fig. 7 were collected by the same 1 MHz broad band piezotrans-
ducer fastened by melted wax to the panel at a point 1.5 in. from where
the signal was introduced, either by transducer or laser pulse.

Figures 8 to 10 show acousto-ultrasonic signals collected from the
graphite/polymer unidirectional 30 ply panel. As with the neat resin,
all the signals were collected by a 1 MHz broad band piezotransducer
fastened by wax to the panel at a point 3.8 cm from, and on the same
side as, where the ultrasonic signal was introduced. Signals were col-
lected with the point of introduction to 1 MHz receiver line parallel
to the fiber direction and also with it perpendicular to the fibers.

Figures 8(a) and (b) show a signal produced with a 2.25 MHz transducer
aligned with the receiver parallel to the fiber direction. Figures 8(c)
and (d) are for the transducers aligned perpendicular to the fibers.

Figures 9(a) and (b) show a signal produced by the lowest laser pulse
energy setting available. The 0.032 J/cm^2 target spot was aligned with
the receiver parallel to the fiber direction. For Figs. 9(c) and (d)
the lowest energy setting gave a 0.029 J/cm^2 pulse. The target spot
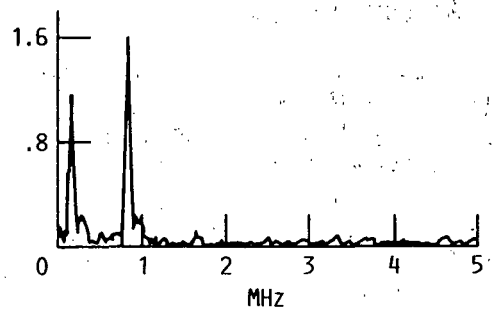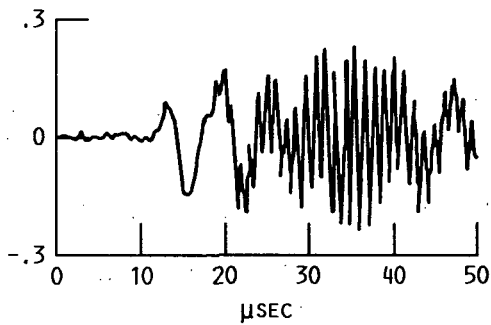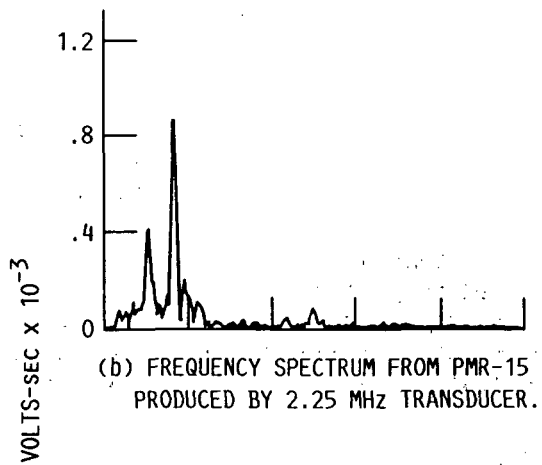was, in this case, aligned perpendicular to the fiber direction.

(a) SIGNAL FROM PMR-15 PANEL PRO-
    DUCED BY 2.25 MHz TRANSDUCER.

(b) FREQUENCY SPECTRUM FROM PMR-15
    PRODUCED BY 2.25 MHz TRANSDUCER.

(c) SIGNAL FROM PMR-15 PANEL PRO-
    DUCED BY 0.03 J/cm^2 LASER
    PULSE.

(d) FREQUENCY SPECTRUM FROM PMR-15
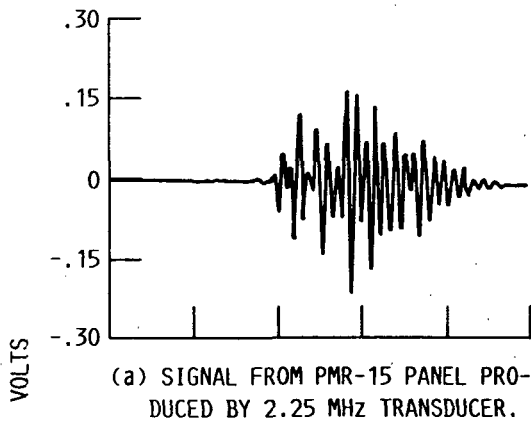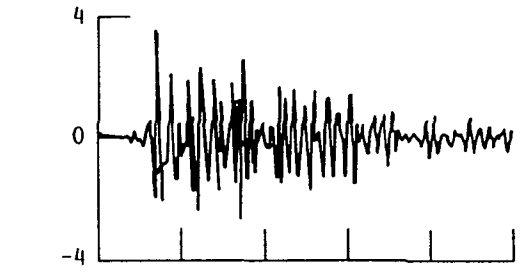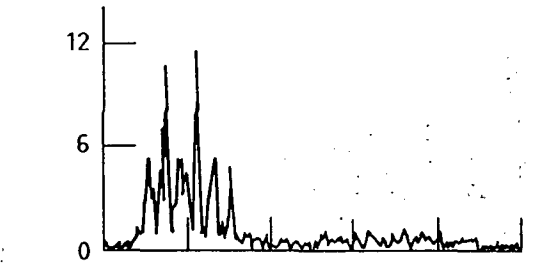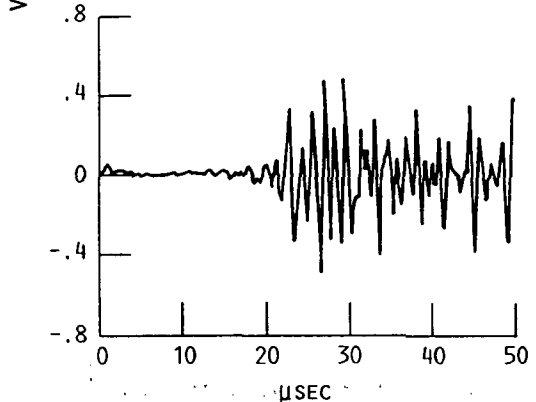   PRODUCED BY 0.03 J/cm^2 LASER
    PULSE.

FIGURE 7. - ACOUSTO-ULTRASONIC SIGNALS COLLECTED FROM PMR-15 PANEL STIMULATED
2.25 MHz TRANSDUCER AND ALSO BY 0.033/cm^2 LASER PULSE.
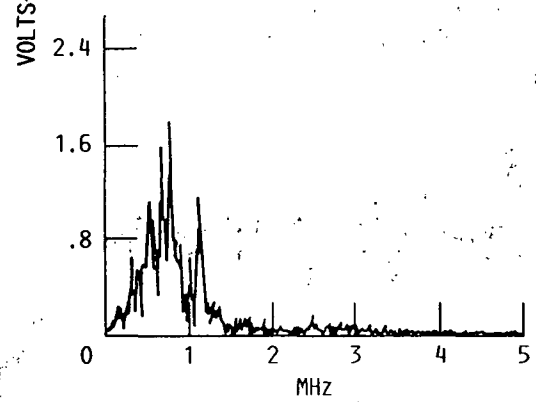
10

(a) SIGNAL PRODUCED ON UNIDIREC-
TIONAL COMPOSITE BY 2.25 MHz
TRANSDUCER PARALLEL TO FIBER
DIRECTION.

(b) FREQUENCY SPECTRUM OF PART (a).

(c) SIGNAL PRODUCED ON UNIDIREC-
TIONAL COMPOSITE BY 2.25 MHz
TRANSDUCER PERPENDICULAR TO
FIBER DIRECTION.

(d) FREQUENCY SPECTRUM OF PART (c).

FIGURE 8. - SIGNALS PRODUCED ON UNIDIRECTIONAL GRAPHITE/POLYMER COMPOSITE BY 2.25
MHz SENDING TRANSDUCER.
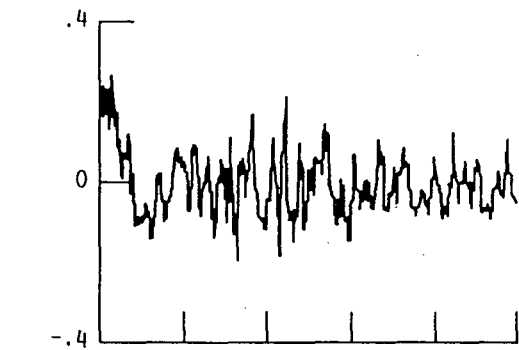
(a) SIGNAL PRODUCED ON UNIDIREC-
TIONAL COMPOSITE BY 0.032
J/CM^2 LASER PULSE COLLECTED
PARALLEL TO FIBERS.

(b) FREQUENCY SPECTRUM OF PART (a).
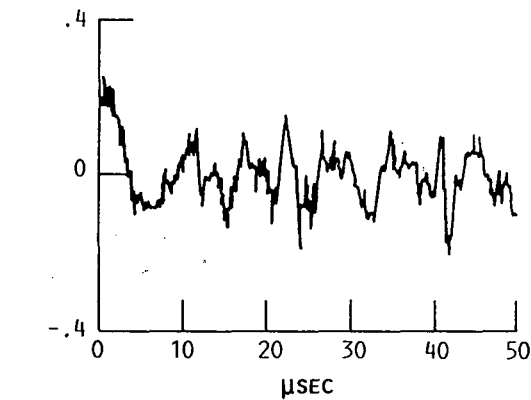
(c) SIGNAL PRODUCED ON UNIDIREC-
TIONAL COMPOSITE BY 0.029
J/CM^2 LASER PULSE COLLECTED
PERPENDICULAR TO FIBERS.

(d) FREQUENCY SPECTRUM OF PART (c).

FIGURE 9. - SIGNALS PRODUCED ON UNIDIRECTIONAL GRAPHITE/POLYMER COMPOSITE BY LASER
LASER AT LOW PULSE ENERGY.

(a) SIGNAL PRODUCED ON A UNIDIREC-
TIONAL COMPOSITE BY 0.234 J/cm^2
LASER PULSE COLLECTED PARALLEL
TO FIBERS.

(b) FREQUENCY SPECTRUM OF (a).

(c) SIGNAL PRODUCED ON A UNIDIREC-
TIONAL COMPOSITE BY 0.197 J/cm^2
LASER PULSE COLLECTED PERPEN-
DICULAR TO FIBERS.
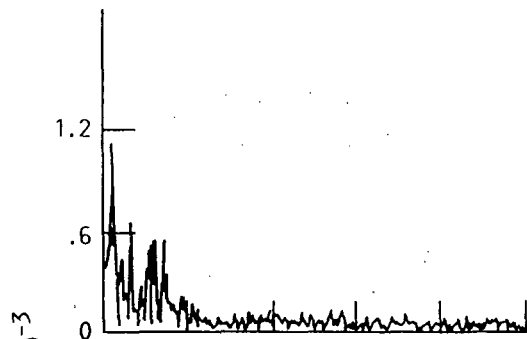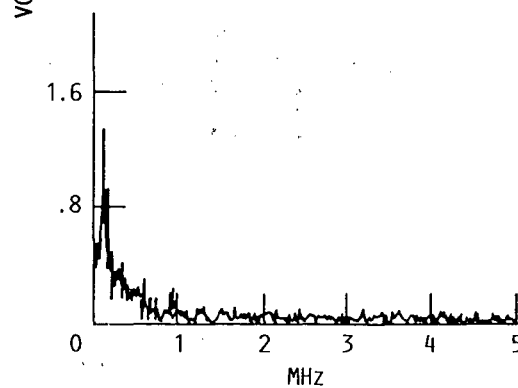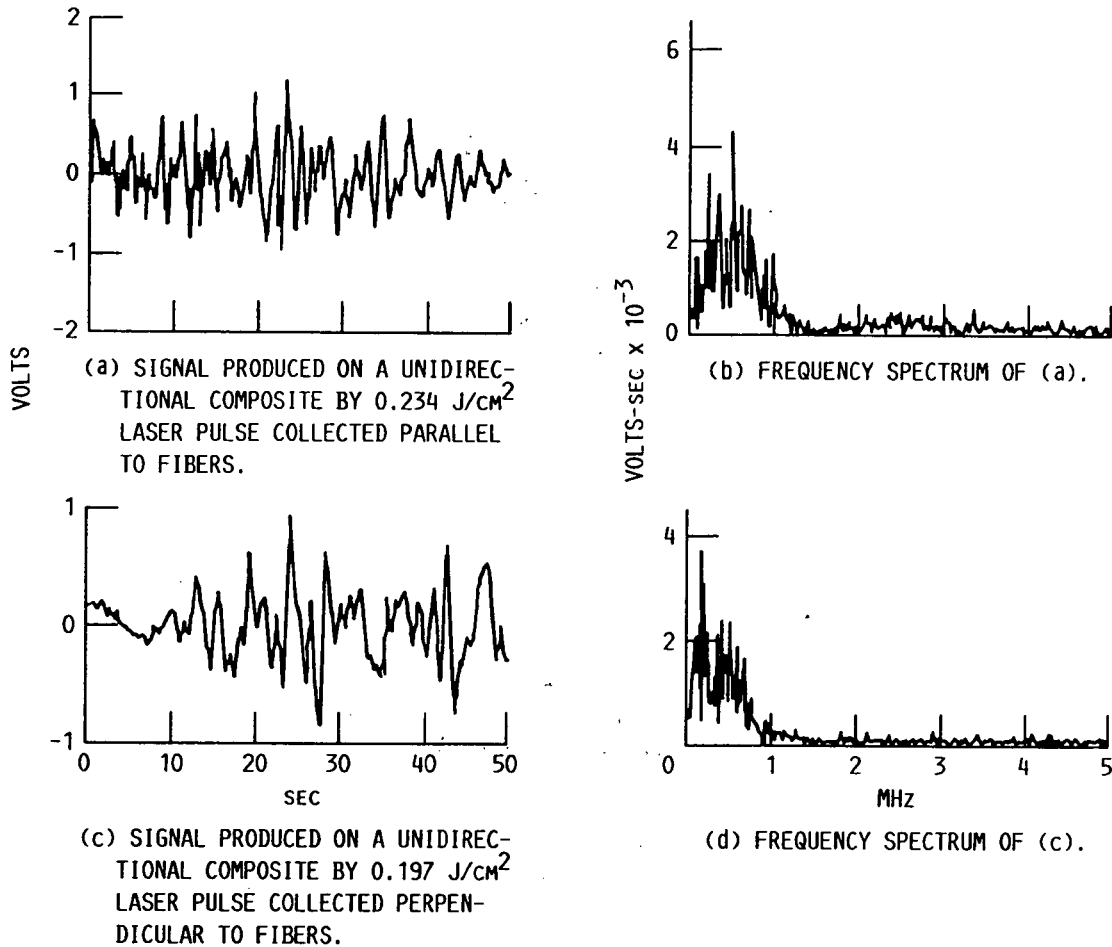
(d) FREQUENCY SPECTRUM OF (c).

FIGURE 10. - SIGNALS PRODUCED ON UNIDIRECTIONAL GRAPHITE/POLYMER COMPOSITE BY
LASER AT HIGH PULSE ENERGY.

Figures 10(a) and (b) show a signal produced by the highest laser pulse
energy setting available. The 0.234 J/cm^2 target spot was aligned with
the receiver parallel to the fiber direction. For Figs. 10(c) and (d)
the highest energy setting gave a 0.197 J/cm^2 pulse. The target spot
was aligned perpendicular to the fiber direction.

Linear stress-wave factors were calculated from the waveforms collected
in these experiments. The linear stress-wave factor, (SWF), is defined
as:

$$SWF = \int_{t1}^{t2} V_{ab}(t)dt \qquad (5)$$

$V_{ab}(t)$ is the absolute value of the amplified receiver output voltage at
time t. t1 and t2 are the beginning and end of the time record of the
acousto-ultrasonic signal collected.

Figure 11 shows plots of linear SWF versus laser pulse energy for the
energy settings available in these experiments. Figure 11(a) is for the
signals produced on a PMR-15 neat resin panel. Figure 11(b) is for the

13
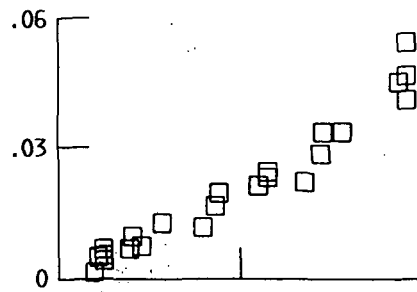
(a) SWF VERSUS PULSE ENERGY
FOR RESIN.

STRESS WAVE FACTOR, VOLTS-SEC
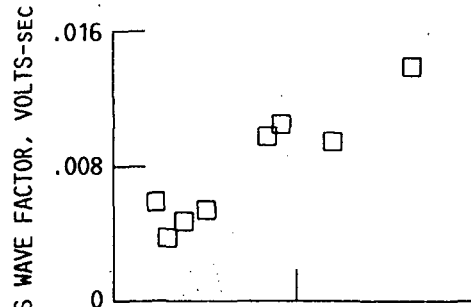
(b) SWF VERSUS PULSE ENERGY FOR
COMPOSITE WITH SIGNAL PATH
PARALLEL TO FIBERS.

LASER PULSE ENERGY, J/CM^2
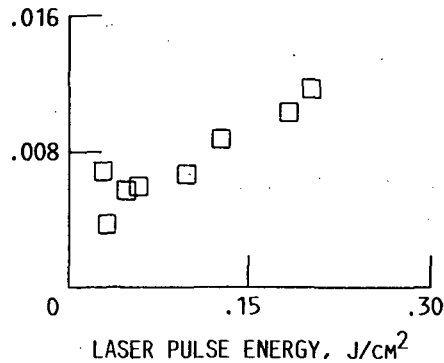
(c) SWF VERSUS PULSE ENERGY FOR
COMPOSITE WITH SIGNAL PATH
PERPENDICULAR TO FIBERS.

FIGURE 11. - STRESS WAVE FACTOR
VERSUS LASER PULSE ENERGY.

unidirectional composite with signal path parallel to the fiber direction. Figure 11(c) is for the unidirectional composite with signal path perpendicular to the fiber direction.

All the acousto-ultrasonic waveform data presented is for geometries with the receiving transducer oriented on the same side of the panel as the ultrasonic energy source. Measurements were also made with the receiver on the opposite side from the source and offset 1.5 in. In the case of the neat resin panels, signals were recovered from the opposite side that were similar in strength as on the same side. In the case of the composites, however, the opposite side signal was greatly reduced in strength from that recovered from the same side.

14

FIGURE 12. - LASER PRODUCED STRESS WAVE FACTOR
DIVIDED BY TRANSDUCER PRODUCED STRESS WAVE
FACTOR VERSUS LASER PULSE ENERGY.
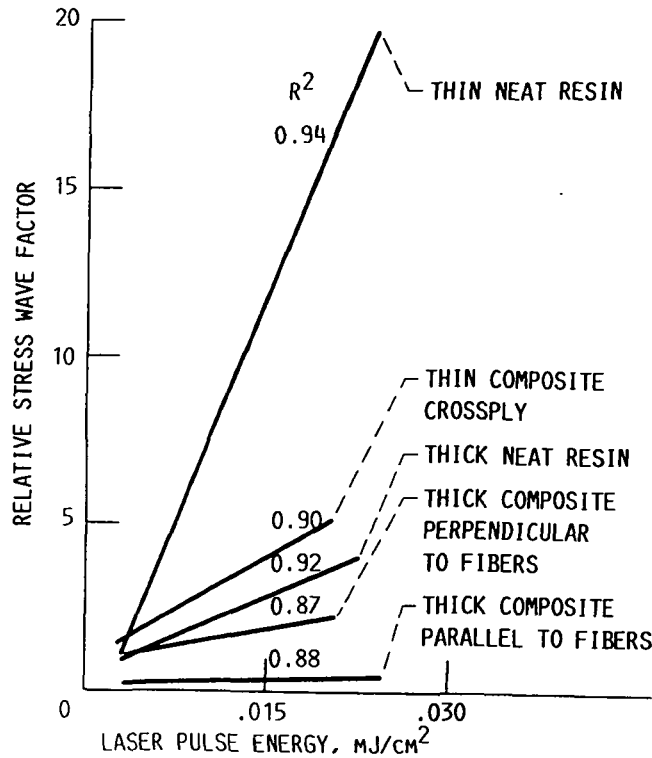
DISCUSSION

Laser Damage Experiments

Earlier studies of laser damage to polymers indicate that two mechanisms
are possible (Refs. 8 to 10). One is photothermal and the second is pho-
tochemical. The photochemical mechanism, photon breaking of molecular
bonds, is not possible at the relatively low photon energy at the NdYAG
1.064 μm wavelength. This leaves the photothermal effect of heating the
material at the site of laser beam incidence to account for our results.

Figures 3 and 4 shows laser damage to a neat resin panel. These photos
show the pitting that occurs at the center of the laser spot as well as
the presence of bubbles under the surface that imply some gas evolution.
(The bubbles are particularly evident in the 200X view of Fig. 4.)
Being black and white, the photos do not show the yellowish discolora-
tion of the damage area. This discoloration, like the other manifesta-
tions, lessens with decreasing energy per pulse. The discoloration
probably indicates the presence of charring of the polymer. Gas evolu-
tion and charring are two signs that decomposition is taking place along
with vaporization. It should be pointed out that these damage sites are
much smaller than the laser beam diameter. The beam diameter is
actually about twice the width of these photos.

As Table 2 shows, in some cases trains of five laser pulses were used
where as in other cases they were single pulses. Single pulses were
separated in time by at least 2 sec. Adjacent pulses in a train were
separated about 10 μsec. There is no difference in the total damage

15

caused by pulses 10 μsec apart from those separated by 2 sec. This implies that the heating of a pulse has effectively dissipated in 10 μsec. If this were not so one would expect that experiments employing pulse trains to cause the material to reach higher temperatures and thus greater damage.

Decreasing individual pulse energy level leads to decreasing damage even though the accumulated energy incident on all the spots is the same. This means that the damage per increment of energy decreases with pulse level. This implies that a damage threshold pulse energy exists. The photos indicate that this threshold is probably between 0.06 and 0.07 J/cm^2. The 0.06 J/cm^2 photos show no sign of damage.

Figure 5 shows that damage in the graphite/polymer composite is much greater than in the neat resins. The primary effect in the composite is the vaporization or burning of graphite fibers. The area affected is much larger than for the resins with the same laser pulse energy. The fibers apparently absorb the laser energy much more than the resin and rise to much higher temperatures. In addition to vaporizing or burning graphite at the center the heat vaporizes the surface layer of resin over a very large area. On the other hand, resin below the surface seems to be shielded. No bubbles or yellow discoloration was observed with the composite. The composite panel in Fig. 5 is a 0/90 cross ply. The greatest damage shown, in Fig. 5(a), does not appear to penetrate to the second ply. This makes the depth <0.02 cm. The width of the fiber burn area is about 0.08 cm. Thus the depth to width ratio for the crater is <1 to 4. This is in contrast to monolithic materials where deep craters are usually found (Ref. 9).

Energy Balance Experiments

The transmission and absorption coefficients found for PMR-15 are estimates. Although the energy ratio E(out)/E(in) reproduces within 3 to 4 percent at one point on one specimen it may vary more than that from place to place. There are visible variations in color and roughness which are probably comparable to variations in the infrared reflecting properties of the materials. The line drawn in Fig. 6 is based on the data for PMR-15. The PMR-11 data point does not fall on this line. It is not obvious whether this represents a difference in infrared properties between the two polymer systems or simply a display of the scatter among three data point.

Of greater significance is the fact that graphite/polymer composites in the same thickness range transmitted pulse energy levels that were below detectability. This is in agreement with the laser damage experiments where there were indications of very strong absorption by graphite fibers very near the surface. This would lead to an absorption coefficient much larger than calculated for the neat resins and therefore a much smaller value of E(out). The rate in which infrared is absorbed is apparently so different between graphite fibers and polymer resin that the exponential decay model may not be appropriate in the composite case.

Note in Eq. (4), that if the attenuation coefficient, α, is large E(out) will be insignificant. Also, most of the laser energy absorbed in the specimen will be near the incident surface. Any ultrasonic waves produced by the conversion of laser energy to mechanical energy will

16

appear near that surface simulating the propagation path conditions that result from a piezotransducer coupled at that spot on the surface. On the other hand, a low value of α will favor a large E(out). It will also mean absorption of a significant amount of energy deeper into the bulk of the specimen. Under this condition ultrasonic waves may appear from the bulk of the specimen rather that solely near the surface. The distribution of wave propagation paths in this case may be quite different from the piezotransducer situation.

Acousto-Ultrasonic Experiments

Figures 7 to 10 show typical acousto-ultrasonic signals collected on the specimens of these experiments. There are three cautions associated with comparing transducer produced and laser produced signals. The first is that the triggering of the waveform digitizer is different between the two systems. Thus there is some offset between their time domain positions. The laser produced signals seem to trigger the system 5 to 10 μsec later than do the transducer signals. The second caution is that absolute signal amplitudes ought not be compared. The amplitude in both cases depends upon the amount of ultrasonic energy introduced. But in the laser case one does not know the conversion efficiency between electromagnetic and ultrasonic energy. Certainly the transducer signal amplitudes can be varied at will by adjusting the pulser settings and the laser pulse can also be adjusted with some range. The third caution is associated with the means of mounting the specimens. For laser measurements they were clamped in one spot in a vertical orientation. For sending transducer they were held horizontally against a corrigated backing sheet by transducer pressure as described in Ref. 6. Boundary conditions for the plate wave component of the signal may have been different for the two orientations.

With the above in mind, we continue by observing that laser produced signals exhibit lower frequency spectra. In the case of the neat resin there is a distinct bimodal spectrum. The high frequency component is much like the spectrum produced by transducer. The laser signal has a different low frequency in the spectrum.

Figures 8 to 10 each show contrasts between wave paths parallel to and perpendicular to the graphite fiber orientation in the unidirectional composite. The transducer produced signals show the early arriving higher frequency component in the parallel signal and absent in the perpendicular measurement. This is in agreement earlier studies (Ref. 6).

The laser produced signals are much less distinct. However, the parallel orientation signals do have higher frequency components that are, again, absent from the perpendicular to fibers signal.

The neat resins exhibit significant through transmission acousto-ultrasonic signals and the composites do not. This is in agreement with the damage and energy balance results. Certainly with the neat resin absorbing laser energy deep in the bulk it will have bulk waves that can be observed on the back side. On the other hand, the composites absorbed laser energy very near the front surface. This apparently favors surface waves that do not appear in the back.

Figure 11 shows that the linear stress wave factor calculated with Eq. (5) for the various specimens is generally linear with laser pulse

energy. The linear stress wave factor is not, however, an energy function. Substituting the quantity $V(t)^2$ for $V_{ab}(t)$ in Eq. (5) gives a quantity that is proportional to the energy of the acousto-ultrasonic signal. The fact that acousto-ultrasonic energy is not linear with laser pulse energy may be related to the fact that damage is being produced at the higher laser energies. The acousto-ultrasonic energy grows faster than expected with high laser energy. In order to explain this by damage one must assume that energy is released to the ultrasonic pulse from the exothermic decomposition of the organic materials of the specimens.

One way to compare the efficiency of producing laser acousto-ultrasonic waves between different materials is to plot a relative stress wave factor. This is the stress wave factor from the laser pulse divided by the stress wave factor from the 2.25 MHz transducer. This is done in Fig. 12 where, as with Fig. 11, the horizontal axis is laser pulse energy. To avoid confusion only the linear regression lines are shown. (R^2 values are included to indicate the degree to which the actual data agrees with those lines.) It can be seen that thin specimens have higher relative energy transfer efficiencies than thick ones.

Figure 12 also shows that neat resins are more efficient than composites. This probably means the polymers convert laser energy to ultrasonic better than graphite fibers.

The thin neat resin has much higher energy transfer efficiency (from laser to ultrasonic) than the thick specimen. This thin panel is the one that transmitted 24 percent of the laser energy out the back surface. The key to its high efficiency is probably that it absorbs laser energy to a large degree throughout its bulk from front to back. Thus it distributes ultrasonic waves throughout the bulk whereas the other specimens produce ultrasonic waves only near the incident surface where the laser pulse is absorbed.

The lowest efficiency is for the thick composite with wave path parallel to fiber direction. It is so low because it is that it is relative to a large transducer produced stress wave factor. This can be inferred by comparing Figs. 8(a) to (c). The parallel to fiber waveform is much larger than the perpendicular one. On the other hand, comparing Figs. 11(b) to (c), we see that the advantage of the parallel orientation is lost with the laser produced signals. This is another indication that the resin converts laser energy to ultrasonic energy more efficiently than do the fibers.

CONCLUSIONS

The 1.064 μm wavelength pulsed NdYAG laser produces acousto-ultrasonic signals in neat polymer resin and in graphite/polymer composite specimens that are similar to those obtained when employing a piezoelectric sending transducer.

The efficiency of inserting ultrasonic energy into a resin matrix relative to insertion into graphite fibers is much higher for laser produced waves than for the piezoelectric transducer case.

The NdYAG pulsed laser can be adopted to the acousto-ultrasonic NDE of graphite/polymer composites provided that pulse energies are employed that are at or below the energy levels studied in the present work. Higher energies can lead to damage at the laser beam impingement site.

A threshold energy value per pulse exists for the onset of laser damage to a composite or neat resin. For pulse energies greater than the threshold damage accumulates with succeeding pulses. For pulse energies less than the threshold no damage accumulates for repeated pulses. The value of the threshold energy is lower for graphite/polymer composites than for neat resins.

ACKNOWLEDGEMENTS

REFERENCES

1. South, H.M., and Palmer, C.H., Analysis of Two-Beam Interferometry for Bulk Wave Measurements, Appl. Opt., vol. 22, pp. 2854-2859, 1983.

2. Palmer, C.H., Circumventing Laser Relaxation Oscillations in Interferometers, Appl. Opt., vol. 23, pp. 3510-3512, 1984.

3. Drake, A.D., and Leiner, D.C., Fiber-Optic Interferometer for Remote Subangstrom Vibration Measurement, Rev. Sci. Instrum., vol. 55, pp. 162-165, 1984.

4. Bourkoff, E., and Palmer, C.H., Low-Energy Optical Generation and Detection of Acoustic Pulses in Metals and Nonmetals, Appl. Phys. Lett., vol. 46, pp. 143-145, 1985.

5. Burger, C.P., Dudderar, T.D., and Gilbert, J.A., Thermal Acoustic Optic NDE for Non-Contact Inspection in Remote Locations, Presented at the Acousto-Ultrasonics: Theory and Application Conference, Blacksburg, VA, July 12-15, 1987.

6. Kautz, H.E., Ray Propagation Path Analysis of Acousto-Ultrasonic Signals in Composites, Presented at the Acousto-Ultrasonics: Theory and Application Conference, Blacksburg, VA, July 12-15, 1987.

7. Von Hipple, A.R., Dielectrics and Waves, John Wiley and Sons, New York, 1954.

8. Garrison, B.J., and Srinivasan, R., Laser Ablation of Organic Polymers: Microscopic Models for Photochemical and Thermal Processes, J. Appl. Phys., vol. 57, pp. 2909-2914, 1985.

9. Braren, B., and Srinivasan, R., Optical and Photochemical Factors Which Influence Etching of Polymers by Ablative Photodecomposition, J. Vac. Sci. Technol. B, vol. 3, pp. 913-917, 1985.

10. Gorodetsky, G., Kazyaka, T.G., Melcher, R.L., and Srinivasan, R., Calorimetric and Acoustic Study of Ultraviolet Laser Ablation of Polymers, Appl. Phys. Lett., vol. 46, pp. 828-830, 1985.

NASA
National Aeronautics and
Space Administration

Report Documentation Page

1. Report No. NASA TM-101299	2. Government Accession No.	3. Recipient's Catalog No.

4. Title and Subtitle		5. Report Date
New Acousto-Ultrasonic Techniques Applied to Aerospace Materials		
		6. Performing Organization Code

7. Author(s)	8. Performing Organization Report No.
Harold E. Kautz	E-4281
	10. Work Unit No. 535-07-01

9. Performing Organization Name and Address	11. Contract or Grant No.
National Aeronautics and Space Administration Lewis Research Center Cleveland, Ohio 44135-3191	
	13. Type of Report and Period Covered

12. Sponsoring Agency Name and Address	Technical Memorandum
National Aeronautics and Space Administration Washington, D.C. 20546-0001	14. Sponsoring Agency Code

15. Supplementary Notes

16. Abstract

The use of an NdYAG pulsed laser for generating ultrasonic waves for NDE in resin matrix composites was investigated. A study was conducted of the use of the 1.064 μm wavelength NdYAG pulsed laser with the neat, unreinforced resin as well as with graphite fiber/polymer composite specimens. In the case of neat resins it was found that, at normal incidence, about 25 percent of the laser pulse energy is reflected at the incident surface. An attenuation coefficient for the polymide resin, PMR-15 was determined to be ~5.8 np/cm. This means, for example, that for a 1/16 in. panel thickness 24 percent of the incident energy is transmitted through the panel. Under these conditions much of the laser produced ultrasonic wave will originate throughout the bulk of the specimen rather than at the surface in contrast to the case with piezoelectric transducers. It was found in energy balance studies that graphite fiber/polymer specimens attenuate the laser beam more than do the neat resins. The increased absorption is in the graphite fibers. The occurrence of laser induced surface damage was also studied. For the polymer neat resin, damage appears as pit formation over a small fraction of the pulse impact area and discoloration over a larger part of the area. A damage threshold was inferred from observed damage as a function of pulse energy. The 600 °F cured PMR-15 and PMR-11 exhibit about the same amount of damage for a given laser pulse energy. The damage threshold is between 0.06 and 0.07 J/cm^2. In the case of graphite fiber/polymer specimens damage studies showed that the fibers burn away to the extent of partially shielding the resin from pit formation and discoloration. Acousto-ultrasonic signals were collected with a piezoelectric transducer over a wide range of laser pulse energies. It was found that signal strengths typical of those produced by piezoelectric sending transducers can be achieved at laser pulse energies well below the damage threshold.

17. Key Words (Suggested by Author(s))	18. Distribution Statement
Nondestructive testing/evaluation; Ultrasonics; Acousto-ultrasonics; Composites; Lasers damage	Unclassified - Unlimited Subject Category 38

19. Security Classif. (of this report) Unclassified	20. Security Classif. (of this page) Unclassified	21. No of pages 20	22. Price* A02

NASA FORM 1626 OCT 86   *For sale by the National Technical Information Service, Springfield, Virginia 22161

National Aeronautics and
Space Administration

Lewis Research Center
Cleveland, Ohio 44135

FOURTH CLASS MAIL

ADDRESS CORRECTION REQUESTED

NASA